

Progress report FUS/PET/MRI (June 6th 2024)

The last period has been fully devoted to the assembly in Valencia and validation of the PET system. First, the system was validated at i3M (Valencia, Spain) and then, shipped to UVa. Once at UVa, the system was installed and simultaneously tested with both the BRUKER 9.4T MR and the RK-300 FUS device.

1. Components performance:

Before starting the PET insert assembly we tested every component individually (SiPM arrays, scintillators, electronic boards, etc...) to ensure optimal performance.

For the scintillator-SiPM gluing we used optical silicon. To verify the coupling process, each one of the 8 printed circuit boards (PCB), a total of 16 SiPM arrays and 16 scintillators, was tested before and after gluing. In particular, we studied the energy spectra (photopeak gain and energy resolution) and the floodmap quality (compression and uniformity) obtained by acquiring data using an encapsulated ²²Na source. Fig 1 shows the floodmaps obtained after gluing.

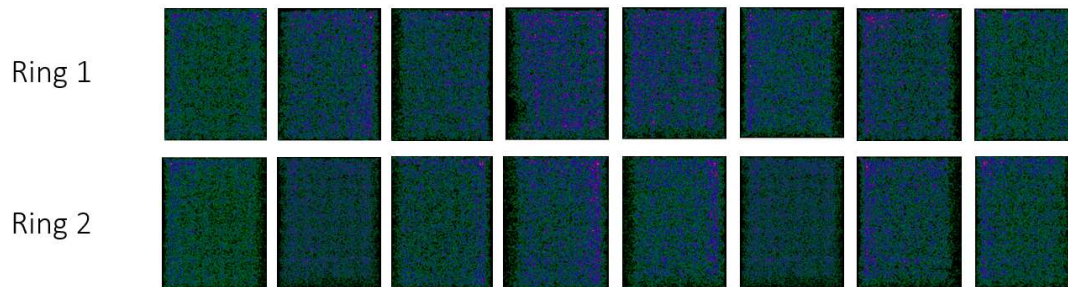


Figure 1. Floodmaps of the 16 crystals measured by placing a point source in the center of the system.

Similarly, the other electronic and mechanical components of the system were validated. These elements include the ADCs, power cables, data transfer cables, power supplies, electrovalve, cooling system (Vortex tubes), to mention but a few. Figure 2 shows the inner part of the assembled cabinet. From left to right, photos of the 8 ADCs mounted on the crate, the compact PCI and power supply; same frontal view but with the frontplane fixed on the ADCs. This photograph also shows custom designed parts for holding the cables and the voltage divider; lateral view of the cabinet where the power supplies and the support for the voltage divisor are fixed, respectively.

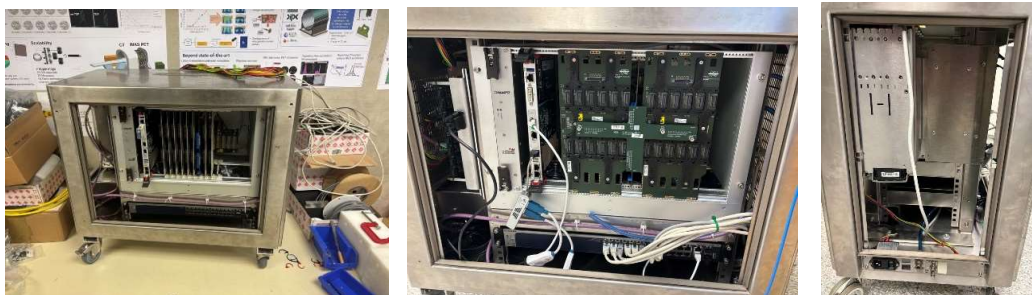


Figure 2. Left, Cabinet with 8 ADCs mounted on the crate, compact PCI and power supply. Center, frontplane fixed on ADCs, cables and support for the voltage divider. Right, lateral view of the cabinet and holder for the voltage divider.

2. System performance at i3M:

Once the individual components were validated, we assemble the system. For this purpose, the set of 8 PCBs, with their respective power supply and data transmission cables, was mounted on a custom designed carbon

fiber structure, thus forming a faraday cage to isolate the system from the MR field. The cables were shielded using a metal mesh and routed to the cabinet where, by means of a specially designed pieces, they were fastened to the cabinet's metal door, thus being isolated from any possible MR interference.

The power cables of each one of the PCBs were connected to the power supplies by means of a voltage divider that allows us to individually regulate each one, thus being able to match the gains of each of the 16 modules. The data transfer cables were plugged to the ADC cards that transform the analog signal coming from the PCBs into digital signals. Then, preliminary tests were carried out by placing an 11x11 array of ^{22}Na at the center of the system. Acquired data was reconstructed as shown in Figure 3.

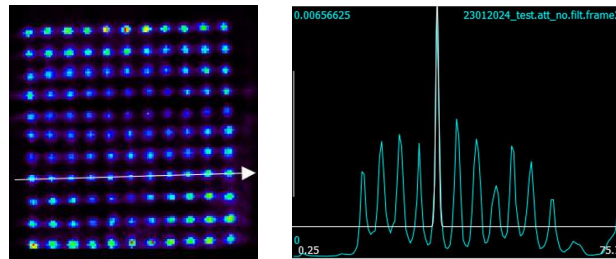


Figure 3. Reconstructed image of the ^{22}Na 11x11 array.

For system calibration and normalization, the system was moved to La Fe Hospital (Valencia, Spain), where we used non-encapsulated ^{18}F -FDG to fill custom designed phantoms. For calibration a fillable phantom of 11x8 wells (sources-like) attached to a tungsten mask was used. Figure 4 Left and Right show the 11x8 wells obtained before and after calibration, respectively. As can be seen the edges decompressed. For system normalization we used a custom designed cylinder than covers the entire FOV.

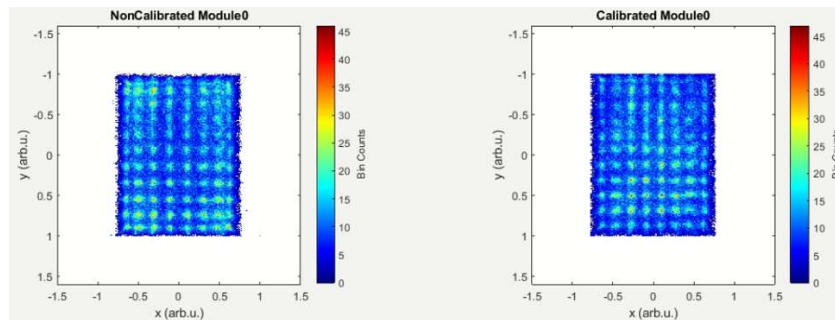


Figure 4. Floodmap of the 11x8 wells phantom before calibration (left) and after calibration (right).

For system performance validation, the measurements detailed in the NEMA NU 4-2008 protocol were carried out. We studied the spatial resolution of the system by placing a ^{22}Na point source at different locations in the FOV. Fig 5. shows the spatial resolution measured at different axial positions at center of the FOV (cFOV) (left) and at 1/4 of the center of the FOV (right).

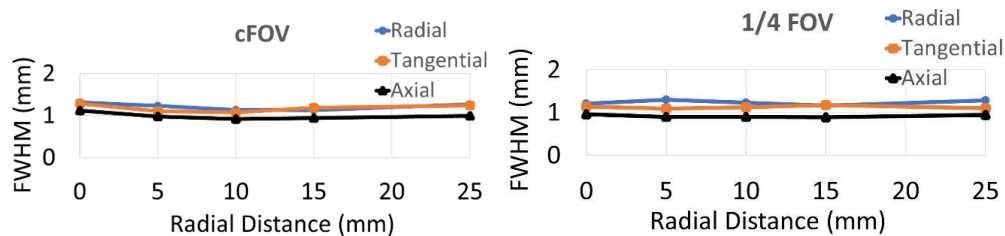


Figure 5. Spatial resolution values measured at different axial positions at center of the FOV (left) and at 1/4 FOV (right).

Figure 6 Left and Right, show the measured sensitivity profiles and Noise Equivalent Count Rate (NECR) achieved, respectively. The sensitivity profiles reached maximum of 3.1% and 3.6% for a 30% and 50% energy windows, respectively. The NECR curve at the 30% energy window indicates that linearity is kept until approximately 92 kcps for an activity of 600 μCi .

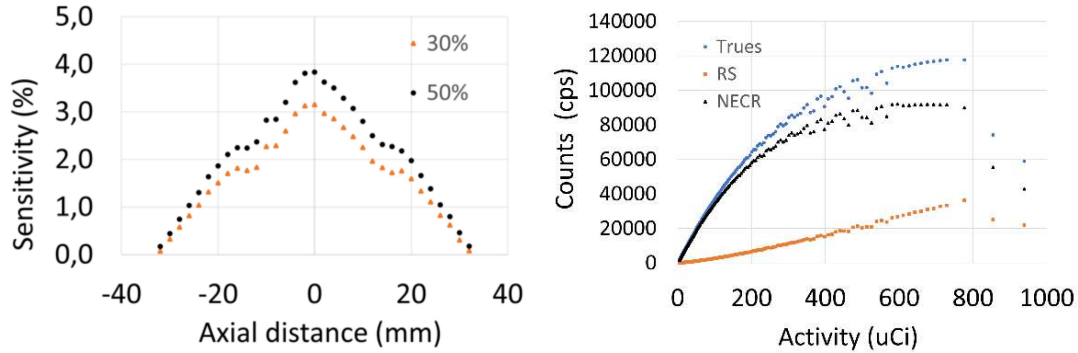


Figure 6. Left, sensitivity profile at 30% and 50% of energy window; Right, NECR, random + scatter and true curves.

Measurements of the Image Quality (IQ) and microDerenzo phantoms were also performed at different activity concentrations. Fig 7. shows the reconstructed images of these phantoms. For the IQ we obtained: (i) Recovery coefficients (RC) of 0.17, 0.38, 0.90, 1.08 and 1.04 for rods ranging from 1 mm to 5 mm in diameter, respectively; (ii) image uniformity of 4.3% and; (iii) spill-over values of 22.9% in water and 15.1% in air. Regarding the microDerenzo, the 0.9 mm rods can be distinguished.

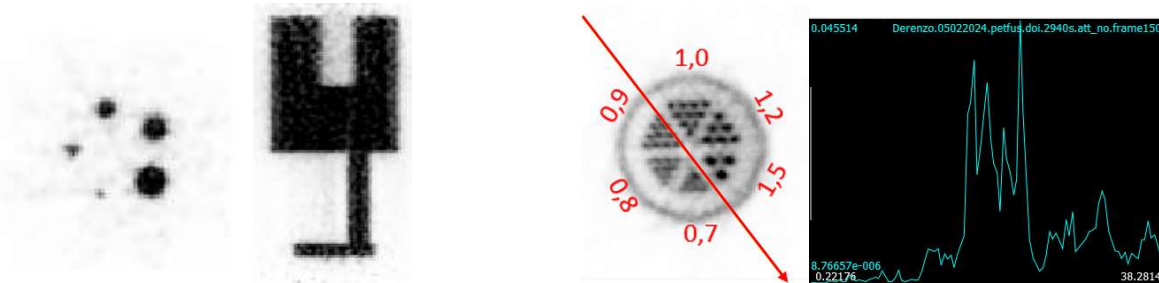


Figure 7. Left, IQ phantom reconstructed (transverse and coronal views). Right, micro-Derenzo phantom with rods size in mm and a line profile through 0,9 mm rods.

3. Transport to UVa, installation and evaluation:

The system was sent to UVa in May 2024. Once the equipment was there, the system was installed and put into operation. Fig. 8 left shows a photo of the system already installed at UVa.

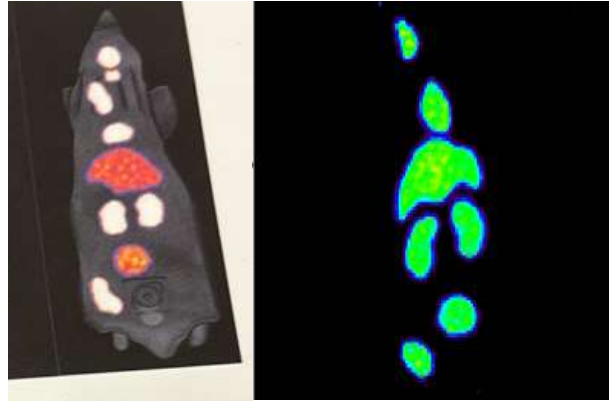


Figure 8. Left. Photograph of the system at UVa. Right, fillable mouse phantom measured with the system.

At UVa, several validation tests were performed by using ^{22}Na sources placed at different positions and also, using the IQ and microDerenzo phantoms. Additionally, a refillable mouse phantom from BIOEMTECH was used. In Figure 8 right, we can see a CT image of this phantom highlighting the fillable cavities (left) and the reconstructed PET image obtained after filling it with ^{18}F .

The system was then transported to the MR room and placed inside the magnet. Simultaneous PET and MR data were acquired by using the IQ and micro-Derenzo phantoms. The MR sequences tested were the TurboRARE, B1 uniformity maps and FLASH. Figure 9 shows the PET inside the MR, and the very preliminary MR and PET images of the IQ phantom obtained with the system working simultaneously.

Note that, to ensure PET/MR compatibility, the IQ and micro-Derenzo phantoms were measured (both phantoms were filled with 89-Zr, 280 micro-Ci and 195 micro-Ci, respectively) when the PET system was outside the MR rooms, inside the MR room but outside the system, inside the MR system but without any gradient being applied (only B0 active) and, inside the MR with different sequences running. These images are being analyzed to study the possible interferences between both systems but so far, no variation in the number of counts or module temperature have been observed.

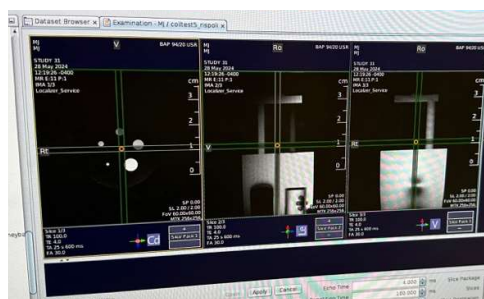


Figure 9. Left, PET system inside the MR. Center and Right, reconstructed MR and PET images of the IQ phantom when both systems were simultaneously working, respectively.

4. PET/FUS/MRI compatibility test:

The designed PET insert aims to be able to operate in parallel with MRI and ultrasound systems. This is why compatibility plays a fundamental role in this validation and assembly phase of the system and must be studied. To validate the capability of the PET scanner to be used as a part of trimodal system,

As part of a tri-modal system, the ability of the PET system to acquire images with an ultrasound probe operating inside it also had to be tested. The commercial FUS device RK-300 already at UVa was used. On

this equipment a mouse previously injected with ^{64}Cu -DOTA, Gd-DOTA and microbubbles was placed on the radiofrequency coil designed in such a way that the ultrasound probe could be focused on the mouse brain, thus allowing the opening of the BBB after sonication.

We carried out one experiment with a mouse. The work flow is described in the following:

- The mouse was sedated and injected with ^{64}Cu -DOTA (200 micro-Ci) + ^{64}Gd Gadolinium. The mouse was placed inside the RF coil and inserted in the PET + MR. PET data was acquired with and without MR sequences running.
- Microbubbles were injected and the sonification process with the FUS device started. PET data was acquired during sonification.
- The FUS stopped and PET + MR data was acquired with and without running sequences.

Figure 10 Shows from left to right: a photo of the mouse in the FUS RF previously to being placed in the PET+MR; MR image of the mouse brain before sonification; and spikes observed when the FUS were being applied. Figure 11 shows the PET and MR images after sonification.



Figure 10. Left. Mouse placed on the RK-300 FUS device before being introduced into the MRI and PET scanners. Center, MR image of the mouse brain before sonification. Right spikes observed when the FUS were being applied.

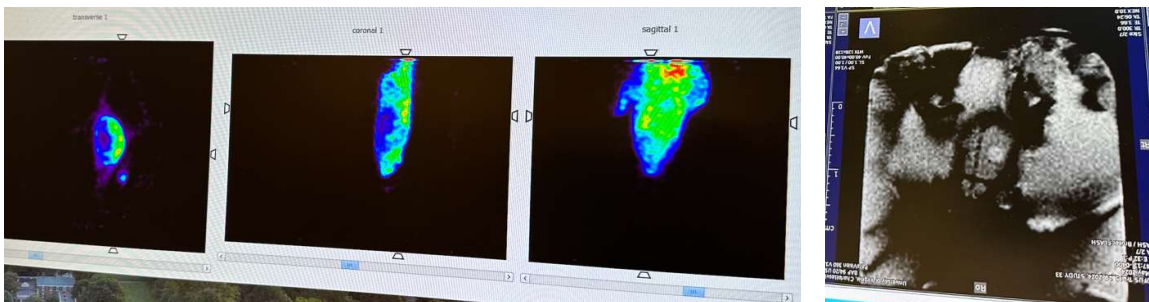


Figure 11. PET and MR images of the mouse after sonification

Antonio J. Gonzalez

June 6th 2024
In Valencia, Spain